A Simplified Expression for Ground Movements Induced by Excavations in Soft Clay

Fuchen Teng(✉)

Department of Civil and Construction Engineering,
National Taiwan University of Science and Technology, Taipei, Taiwan
fteng@mail.ntust.edu.tw

Abstract. Clays are generally known not to be isotropic materials. The inherent anisotropy of clays results from the deposition process, which tends to induce a horizontal bedding plane in the soil layer. Soil movements induced by excavation activities are a crucial issue in urban geotechnical engineering with soft clays. However, empirical and semi-empirical methods for evaluation of lateral soil movements induced by excavations with consideration of inherent anisotropy have not been well-established. This study aims to establish a simplified evaluation for predicting ground movements reasonably based on a soil model which considered small-strain properties and anisotropic behavior. Parametric study by numerical analyses with an anisotropic soil model was used in this study. The anisotropic ratio for soil moduli was one of the factors in the simplified expression and ranged from 1.0 to 1.4 which agreed well with test data on many soft clays. A set of simplified expressions for predicting ground movements is proposed. Only the excavation geometry, the subsoil properties, stiffness of braces, and inherent anisotropy are required to evaluate the ground movements.

Keywords: Excavation · Inherent anisotropy · Soil movement · Simplified expression

1 Introduction

Ground movements induced by excavations generally involve the lateral deflection of retaining structure and settlement of surrounding soils. Adjacent buildings may be damaged when the ground movement is greater than the tolerable value. Thus, the prediction of ground movement near an excavation becomes an important topic in the design of excavation. Finite-element method (FEM) is generally employed to estimate the wall deflections and ground surface settlements. The accuracy of estimation highly depends on the soil constitutive model used in the FEM. Although soil models that considered the small-strain behavior (Whittle and Kavvads 1994; Benz 2007; Hsieh and Ou 2011) and stiffness anisotropy of soil (Teng et al. 2014) are available in recent years. However, observation and selection of soil characteristic such as behaviors at small strain and properties of anisotropy is generally difficult and costly because those properties can only be obtained through specialized tests, which are not

R. Chen et al. (eds.), *Proceedings of the 2nd International Symposium on Asia Urban GeoEngineering*, Springer Series in Geomechanics and Geoengineering,
https://doi.org/10.1007/978-981-10-6632-0_8

available to most of consultants and designers. Therefore, a simple and reasonable assessment on ground movements induced by excavation is desirable and required to examine the design of excavation.

Several empirical and simplified methods (Clough and O'Rourke 1990; Kung et al. 2007; Hsieh 2001) have been developed to predict the maximum wall deflection induced by deep excavation through case histories. Results of those estimations are satisfactory even though the deflection of wall involves complex soil-structure interactions. Nevertheless, the empirical and simplified predictions of ground settlement are relatively unreliable because case histories with observations of ground settlements are very limited. Observation of ground surface settlements adjacent to excavations is often influenced by construction vehicles, dewatering, existing structures nearby, and accuracy of instruments. In addition to case histories, numerical parametric studies can also be used to establish simplified methods for predicting ground surface settlements. To accurately predict the ground surface settlement behind the wall using numerical methods, the constitutive model of soil should be able to reproduce the soil behavior at various strain level and include the non-linear and anisotropic behavior (Pestana and Whittle 1999; Ng et al. 2004; Teng et al. 2014). However, advanced models are seldom used in parametric studies to examine the characteristic of ground settlement.

For determining the maximum ground surface settlement, evaluation methods proposed in several works (Peck 1969; Bowles 1986; Clough and O'Rourke 1990; Ou et al. 1993; Hsieh and Ou 1998; Kung et al. 2007) are often used for estimating the ground surface settlement. Evaluation methods based on field observations, i.e., empirical equations, were highly affected by the accuracy of measurements.

In addition to ground surface settlement, the prediction of ground settlement below the ground surface is also of interest to engineers. As shown in Fig. 1, footings of adjacent buildings are usually placed underground rather than placed on the ground surface. However, the behavior of subsurface settlement, i.e. the shape and magnitude of settlement troughs, is not well investigated. The evaluation of damage potential of buildings adjacent to a braced excavation is dependent on the subsurface settlement profile. Therefore, the ground settlement, which includes subsurface settlement and surface settlement, needs to be properly investigated.

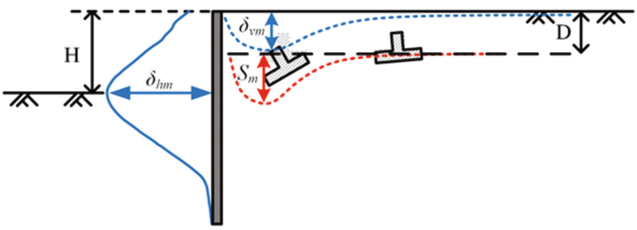

Fig. 1. Schematic diagram for ground movements induced by excavation

This study aims to establish a simplified method for predicting the excavation induced movement, including the maximum wall deflection (δ_{hm} in Fig. 1), the maximum ground settlement (δ_{hm} in Fig. 1), and the subsurface ground settlements (S_m in

Fig. 1), induced by deep excavation. Parametric study with an advanced soil model which considers the small-strain behavior and stiffness anisotropy of soils (Teng et al. 2014) was carried out in this study. A large number of FEM analyses of hypothetical cases with different configurations of influence factors such as excavation dimensions, soil strength, structure stiffness, and stiffness anisotropy of soils were employed. Finally, the proposed simplified evaluation methods are validated through comparison with data from 35 excavation case histories.

2 Influence Factors to Ground Movement

Factors that influence ground movements induced by excavation have been studied by various researchers (e.g. Wong and Broms 1989; Clough and O'Rourke 1990; Hashash and Whittle 1996; Hsieh 2001; Kung et al. 2007). These factors include the excavation depth (H), the excavation width (B), the undrained shear strength of the subsoil (s_u) or the factor of safety against basal heave, the system stiffness of the wall (S_w), and the axial stiffness of wall bracing (S_a). According to Clough and O'Rourke (1990), the system stiffness of wall is dimensionless and defined as

$$S_w = \frac{E_w I_w}{\gamma_{wat} h_{avg}^4} \tag{1}$$

where E_w is the Young's modulus of the wall; I_w is the moment of inertia per unit length of the wall; γ_{wat} is the unit weight of water; h_{avg} is the average vertical spacing of lateral struts.

The axial stiffness of the lateral strut per unit length of the wall is defined as

$$S_a = \frac{A_{st} E_{st}}{s} \tag{2}$$

where A_{st} is the average cross sectional area of the lateral struts for each level; E_{st} is the Young's modulus of the lateral strut; s is the horizontal spacing between the lateral struts.

In addition to factors mentioned above, the stiffness anisotropy of soils could affect the ground movement surrounding an excavation. The inherent anisotropy of stiffness was observed in multi-directional bender element tests on several soft clays as listed in Table 1 (Ng et al. 2004; Cho and Finno 2010; Teng et al. 2014). The stiffness anisotropy of clays was generally assumed to be cross-anisotropic since there is a horizontal plane of isotropy, i.e., the bedding plane. The cross-anisotropic constitutive equation is usually used to simulate the anisotropy of soils. Cross-anisotropic soil models have been applied in numerical analyses to predict ground settlements due to tunneling (Lee and Rowe 1989; Simpson and Ng 1995). It has been shown that the use of cross-anisotropic elastic parameters improves the accuracy of predictions of settlement profiles, including the shape and magnitude of settlement troughs, and the predictions agreed well with field observations (Teng et al. 2014). The anisotropic ratio of stiffness is defined as

Table 1. Anisotropy of stiffness for different clays

	Ng et al. (2004)	Cho and Finno (2010)	Teng et al. (2014)
Soil type	Completely decomposed tuff	Chicago glacial clay	Taipei silty clay
Sample type	Intact sample	Intact sample	Intact sample
Anisotropic ratio	1.15–1.36	1.0–1.4	1.15–1.42

$$AR = \frac{G_{hh}}{G_{vh}} \tag{3}$$

where G_{vh} is the shear modulus in the vertical plane; G_{hh} is the shear modulus in the horizontal plane.

Six major factors, i.e., H, B, s_u, S_w, S_a, and AR, that affect ground movements caused by excavation were employed in the parametric study presented herein. The configuration of the parametric study is introduced in the following section.

3 The Fem Parametric Study

3.1 Introduction and Validation of FEM with An-USC

The parametric studies were performed in a finite-element program (PLAXIS 2D) with an advanced soil constitutive model, the anisotropic undrained soft clay moel (An-USC model). The An-USC model which originated from the undrained soft clay model (Hsieh and Ou 2011), is a stress path dependent undrained soil model and based on the concept of effective stress. Both the anisotropy of soil strength, the anisotropy of stiffness, and small-strain behaviors of soils are simulated by the An-USC model. Only eight parameters are required to fully describe the An-USC model: undrained shear strength in axial compression (s_u), Young's modulus at small strain (E_i), failure ratio (R_f), Poisson's ratio (υ), anisotropic ratio of undrained strength (K_s), anisotropic ratio of stiffness (AR), and degradation parameters (m and n). Among these parameters, s_u and R_f are exactly the same as those in the original Duncan-Chang model (Duncan and Chang 1970). The Young's modulus at small strain (E_i) can be obtained from small strain tests, bender element tests or empirical correlations. The anisotropic strength factor (K_s) is obtained from triaxial compression tests and extension tests. The anisotropic ratio of stiffness can be obtained from multi-directional bender element test. Degradation parameters (m and n) can be obtained from unloading-reloading triaxial tests.

The FEM analyses with An-USC model are validated by predicting the excavation-induced ground movements. A well-documented excavation case with field monitoring data and soil testing data (Ou et al. 1998, 2000a, and 2000b) is used to calibrate the FEM solution. The geometry of the excavation site was trapezoid and show in Fig. 2a. The depth of the excavation was 19.7 m, and dimension of diaphragm

wall was 0.9 m thick and 35 m deep. The basement was completed by the top-down construction method, in which the wall was supported by solid concrete floor slabs of 0.15 m thick. Figure 2b shows the comparison of wall deflection and ground surface settlement between field observations and predictions, respectively. Based on the FEM results, An-USC model gave predictions close to field observations on both the maximum wall displacement and the shape of wall deformation curves in all stages. For the ground surface settlement, the prediction was not only accurate on the maximum settlement but also the settlement beyond the location of the maximum settlement. In addition, the location of maximum ground surface settlement was also well predicted. Thus, the accuracy of the FEM with An-USC model is considered satisfactory for the following parametric study.

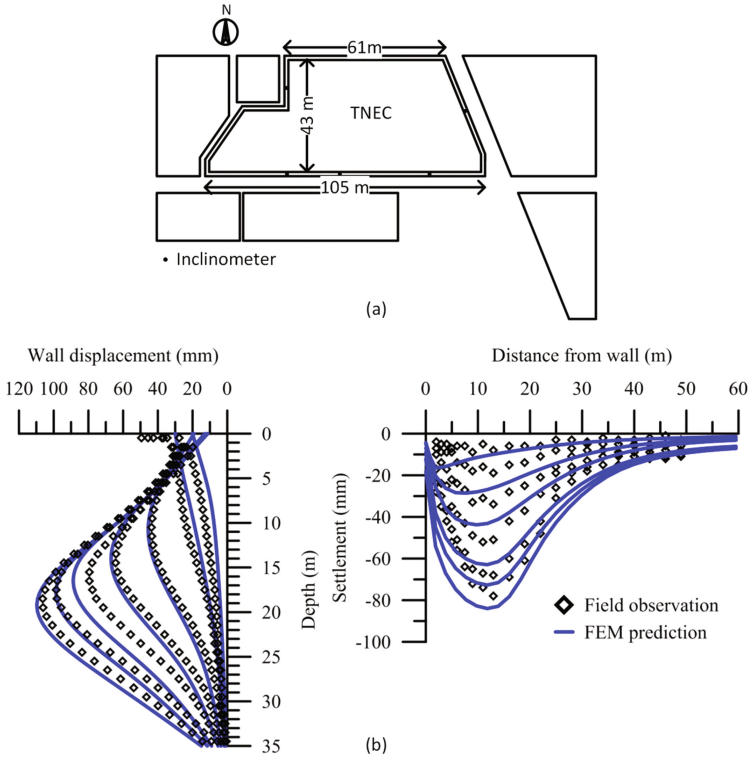

Fig. 2. (a) Geometry of the calibration case, (b) prediction of wall deflection and ground surface settlement by FEM with An-USC model

3.2 Configuration of Hypothetic Excavations

The mesh of hypothetical case used in the parametric study is shown in Fig. 3, in which the excavation was assumed symmetric to the centerline of the excavation width.

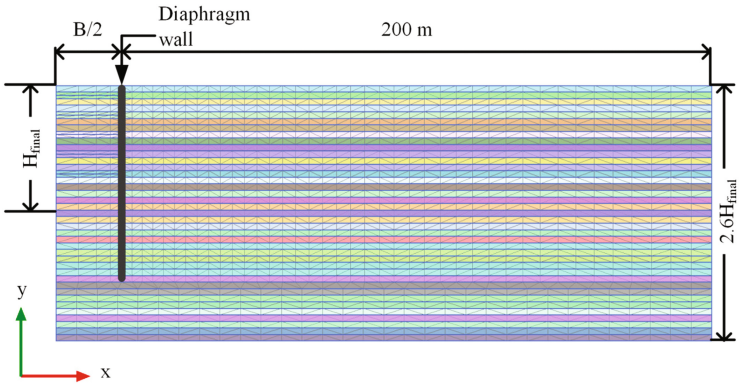

Fig. 3. Mesh in numerical analysis

As shown in the Fig. 3, the left boundary of the finite element mesh is at the center of excavation and the right boundary is at the distance of 200 m from the excavation center, which is sufficiently long for all hypothetic cases. The bottom boundary is at a depth of 2.6 times of the final excavation depth. The length of the wall is equal to twice of the final excavation depth. For the boundary conditions, the boundary of the bottom was restrained from both horizontal and vertical displacements while the left and right boundaries were restrained from the horizontal displacement.

The subsoil was assumed to be a uniform clay layer with a unit weight of 18.24 kN/m^3. The groundwater level was located at the ground surface and in a hydrostatic distribution with the depth. The normalized Young's modulus of the clay at small strain (E_i/σ'_v, where σ'_v is the effective vertical stress) is within the range of 588 to 714. The coefficient of earth pressure at rest (K_O) was assumed to be 0.5. All structures in the analysis such as walls and struts were simulated by linear elastic model. Plate elements were used to model the wall while anchors were used to simulate the lateral struts.

The values of factors that influenced ground movements in the parametric study, i.e., H, B, s_u, S_w, S_a, and AR, were varied as listed in Table 2. Three different final excavation depths, 10 m, 20 m, and 30 m, were employed in the parametric study. Detailed construction sequence of hypothetic excavations is shown in Fig. 4. The lateral strut of each level was installed at a depth of 1.0 m above the current excavation surface. The variation of the factors listed in Table 2 generally covered most of practical excavation cases. Ranges of excavation dimensions, i.e., H and B, are 10 m to 30 m and 20 m to 80 m, respectively. The system stiffness of wall, S_w, started from the flexible to stiff structures. The S_a coved the axial stiffness of steel struts to that of concrete floor slabs. As observed in Table 1, the anisotropic stiffness ratios for soft clays are in the range of 1.1 to 1.4. Therefore, anisotropic ratios of soil stiffness were set as 1.0 (isotropic) to 1.4 herein. A total number of 729 hypothetic excavations were generated based on the variation of the factors in Table 2. Among these 729 artificial cases, some had unrealistic excavation conditions, such as a deep and wide excavation (H : 30 m × B : 80 m) in soft clays but with a soft wall and soft lateral supports.

Table 2. Variation of the factors that used in the parametric study

Factor	Values
H (m)	10, 20, 30
B (m)	20, 40, 80
s_u/σ'_v	0.28, 0.3, 0.34
S_w	352, 1760, 5280
S_a (MN/m)	550, 2960, 11830
AR	1.0, 1.2, 1.4

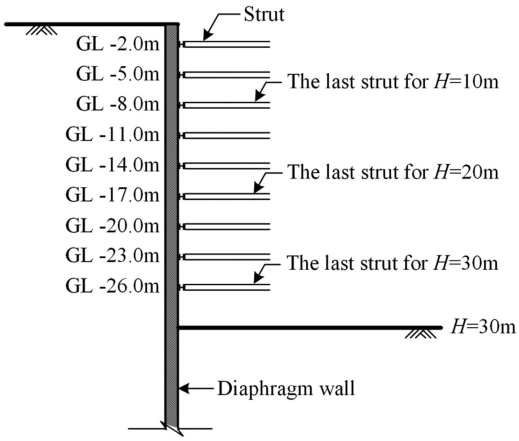

Fig. 4. Construction sequence of the hypothetical excavation

By excluding such unreasonable cases, the total number of FEM analyses is thus reduced to 180, which will be used to establish a simplified evaluation method for excavation-induced ground movements.

4 Simplified Methods for Predicting Ground Movements

4.1 Determination of the Maximum Wall Deflection

Results of FEM numerical analyses of 180 artificial excavations were collected and used to obtain the relationship between maximum wall deflections (δ_{hm}) and factors of influence (H, B, s_u, S_w, S_a, and AR). By applying the multivariate regression analysis on the results and the parameters, the normalized maximum wall deflection, δ_{hm}/H, could be calculated by equations below:

$$\delta_{hm}/H = 0.09\exp(78.03X_{e,hm}) \tag{4}$$

$$X_{e,hm} = 3.05 \times 10^{-4} H + 1.53 \times 10^{-4} B - 0.124 s_u / \sigma'_v - 1.49 \times 10^{-6} S_w - 2.63 \times 10^{-7} S_a - 2.25 \times 10^{-3} AR \quad (5)$$

where $X_{e,hm}$ is a synthetic parameter for determining the maximum wall deflection which takes all factors of influence such as excavation geometry, subsoil properties, and stiffness of braces into consideration. The units of parameters in Eq. (5): H and B are in meter; S_a is in MN/m; s_u/σ'_v, S_w, and AR are dimensionless. δ_{hm} from FEM analyses, $X_{e,hm}$ calculated by Eq. (5) based on parameters listed in Table 2, and the regression curve are shown in Fig. 5. The coefficient of determination, R^2, of the regression curve in Fig. 5 is 0.81.

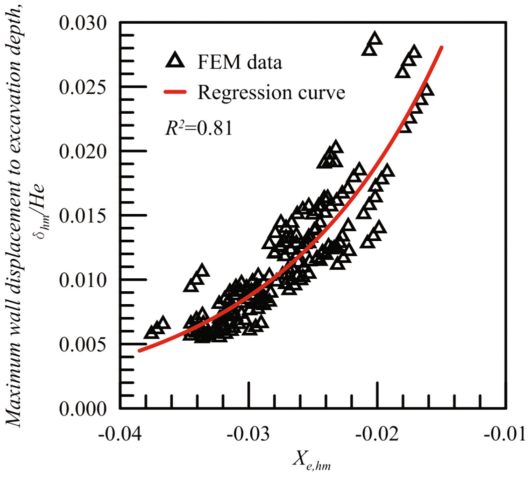

Fig. 5. Relationship between the ratio of the maximum wall deflection to the excavation depth and $X_{e,hm}$

According to the work by Hsieh (2001), the wall deflection will increase with the increase of the depth of a hard stratum, H_g, measured from the ground surface. When the H_g/H is greater than or equal to 1.8 which implies the hard stratum is sufficiently deep, the wall deflection is not affected by the existence of the hard stratum. However, for the situation that H_g/H is less than 1.8, the hard stratum will restrain the wall deflection induced by excavation. A modification factor, α_g, is proposed as

$$\alpha_g = 0.91 \frac{H_g}{H} - 0.64 \leq 1.0 \quad (6)$$

The proposed simplified equation for estimating the wall deflection is based on the parametric study on FEM in which the bottom boundary, i.e., the hard stratum, is located at a depth of 2.6H. Therefore, the Eq. (4) is applied to excavations with $H_g/H \geq 1.8$ only.

For excavations with shallower hard stratum, i.e., $H_g/H < 1.8$, the maximum wall deflection calculated by Eq. (4) should multiply the modification factor α_g.

The system stiffness of the wall, S_w, in Eq. (5) is usually related to the final excavation depth. In practice, a stiffer wall is designed for an excavation with deeper final excavation depth. Hsieh (2001) suggested the relationship between the system stiffness of the wall (S_w) and the final excavation depth (H_{ef}) by observing field data as

$$S_w = 98.02H_{ef} - 32.39 \tag{7}$$

The stiffness of the strut, S_a, is also related to the final excavation depth. Usually, a stiffer strut is designed for a deeper excavation. The relationship between S_a and H_{ef} was obtained on several case histories as shown in Fig. 6. The relationship is as follows:

$$S_a = 91.45H_{ef} - 515.9 \tag{8}$$

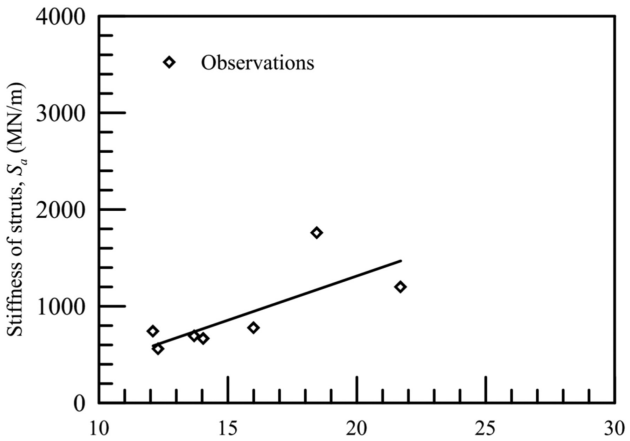

Fig. 6. Relationship between S_a and H

By substituting Eqs. (7) and (8) into Eq. (5), the calculation of parameter $X_{e,hm}$ could be reduced as an equation with only four parameters, i.e., H_{ef}, B, s_u, and AR. For most of normally consolidated clay, the AR can be assumed to be 1.2. Therefore, a quick evaluation method for the maximum wall deflection is proposed. Figure 7 shows such a relationship for soft clay ($s_u/\sigma'_v = 0.28$) and medium clay ($s_u/\sigma'_v = 0.34$). Each of the curve in the figure, namely linear, corresponding to a value of B can be approximated by a specific ratio of δ_{hm} to H_e. For a specific area of soils, for example,

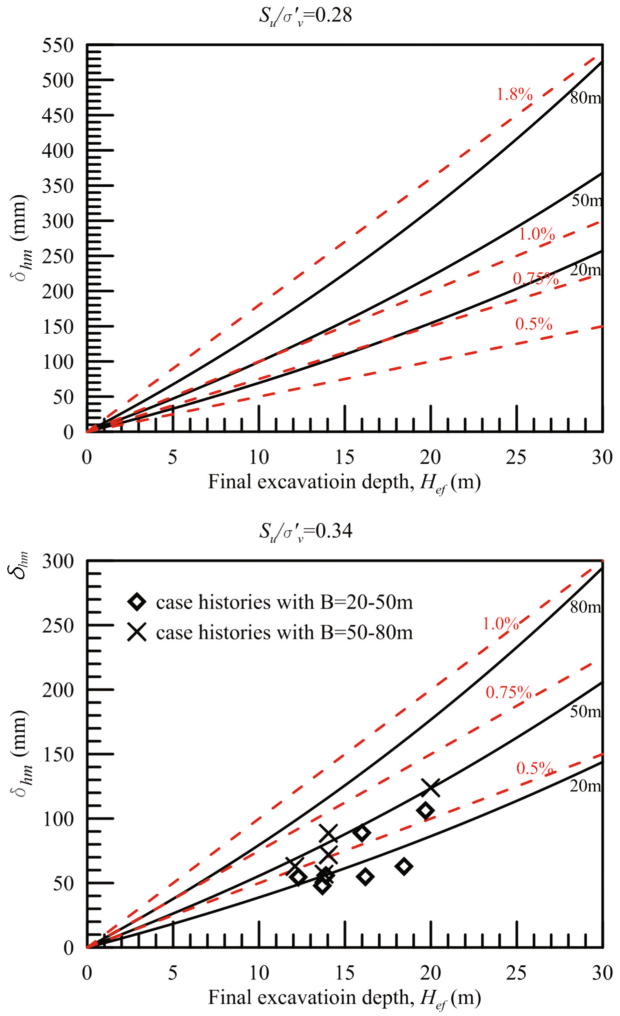

Fig. 7. Evaluation for the maximum wall deflection based on H_{ef}

$s_u/\sigma'_v = 0.28$, with a known B = 50 m and H_e = 20 m, an approximate line of $\delta_{hm}/H_e \cong 1.1\%$ can be selected as a first assessment, and therefore, the initial estimation for δ_{hm} would be 220 mm.

4.2 Determination of the Maximum Ground Surface Settlement

The maximum ground surface settlements, δ_{vm}, obtained from the FEM analyses were also used to derive the simplified evaluation equation. The relationship between the maximum ground surface settlement (δ_{vm}) and factors of influence (H, B, s_u, S_w, S_a, and AR) is obtained by applying the multivariate regression analysis on the results and the

parameters. The normalized maximum ground surface settlement, δ_{vm}/H, could be calculated by

$$\delta_{vm}/H = 0.102\exp(106.19X_{e,vm}) \tag{9}$$

$$X_{e,vm} = 1.78\times10^{-4}H + 1.14\times10^{-4}B - 0.102s_u/\sigma'_v - 1.1\times10^{-6}S_w - 2.23\times10^{-7}S_a - 1.54\times10^{-3}AR \tag{10}$$

where $X_{e,vm}$ is a synthetic parameter for determining the maximum ground surface settlement, inclusive of excavation geometry, soil properties, and stiffness of braces. Figure 8 shows the numerical data of δ_{vm} and $X_{e,vm}$ and the regression curve where $R^2 = 0.8$.

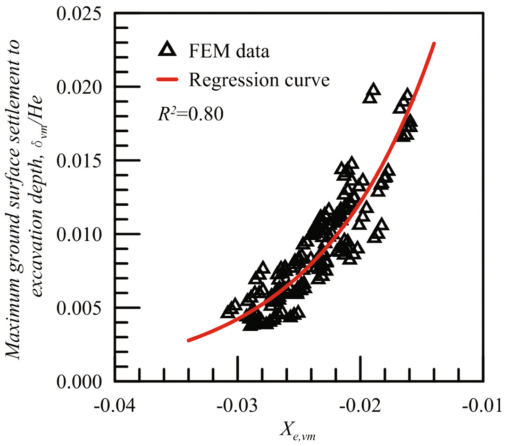

Fig. 8. Relationship between the ratio of the maximum ground surface settlement to the excavation depth and $X_{e,vm}$

The Eq. (10) could be also reduced by Eqs. (7) and (8), and resulted in the quick evaluation for estimating the maximum ground surface settlement without the parameter of S_w and S_a. Figure 9 shows the relationship between δ_{vm} and the H_e for soft clay ($s_u/\sigma'_v = 0.28$) and medium clay ($s_u/\sigma'_v = 0.34$). Similarly, for $s_u/\sigma'_v = 0.28$, with the known B = 50 m and H_e = 20 m, an approximate line of $\delta_{vm}/H_e \cong 0.8\%$ can

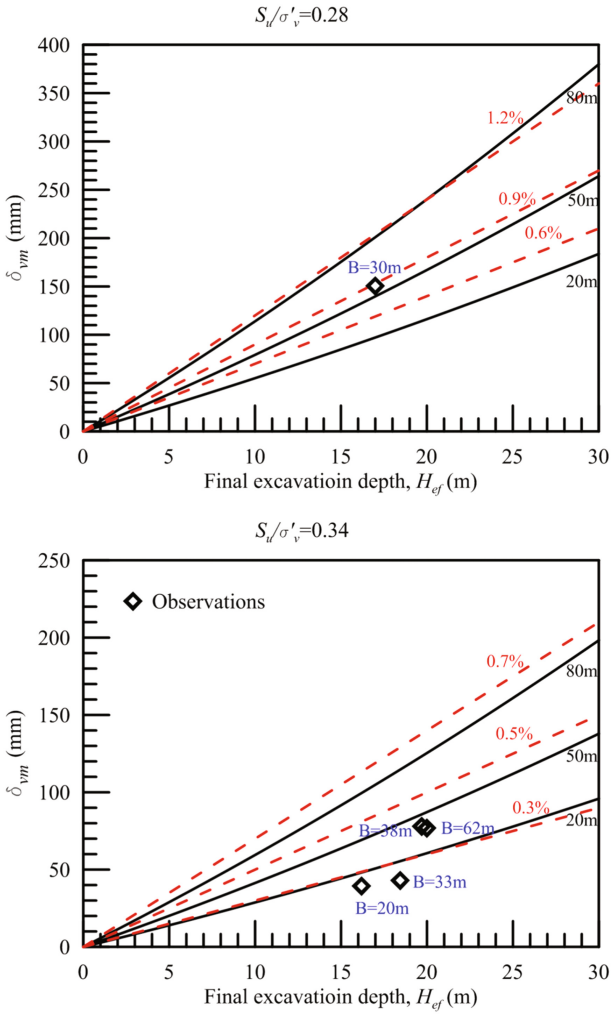

Fig. 9. Evaluation for the maximum ground surface settlement based on H_{ef}

be selected as a first assessment, and therefore, the initial estimation for δ_{vm} would be 160 mm.

The ground surface settlement can be determined directly from Eqs. (9) and (10), which based on the influence factors. However, for those situations that reliable maximum wall deflections were known, the ground surface settlement can also be determined by the relationship between δ_{vm} and δ_{hm}. Results from numerical analyses on hypothetic excavations were used to establish the relationship between δ_{vm} and δ_{hm}. Figure 10 shows the maximum ground surface settlement against the maximum wall

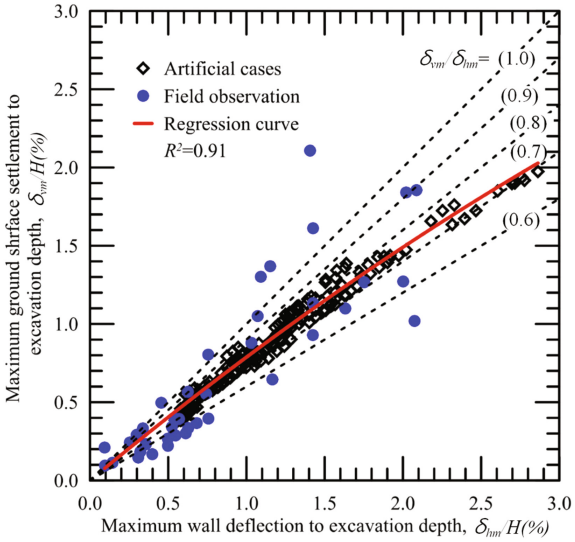

Fig. 10. Relationship between max ground surface settlement and max wall deflection

deflection either from FEM analyses or field observations. For the generated excavation data, the ratios of the maximum ground surface settlement to the maximum wall deflection were generally located within the range of 0.7 to 0.9. While the δ_{vm}/δ_{hm} is more scattered for field observations. The regression equation shown in Fig. 10 is as follows.

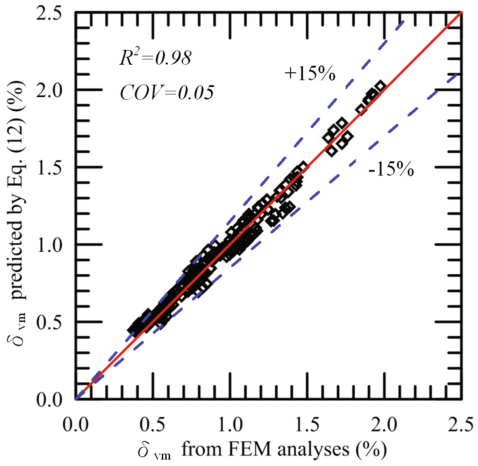

Fig. 11. Performance of Eq. (11) in predicting the ground surface settlement for hypothetical cases

$$\frac{\delta_{vm}}{H} = -0.04\left(\frac{\delta_{hm}}{H}\right)^2 + 0.82\frac{\delta_{hm}}{H} \tag{11}$$

Figure 11 shows the performance of Eq. (11) in reproducing the results of FEM analyses. As observed in the figure, the prediction made by Eq. (11) is consistent with results calculated from FEM analyses. The high R^2 value (0.98) and low coefficient of variance (COV = 0.05) illustrates that the accurate maximum ground surface settlement could be obtained if a reliable maximum wall deflection is known. In addition, most of data points shown in the figure were located in the range of ±15% of the line where predicted δ_{vm} is equal to δ_{vm} from FEM. Further validations of Eq. (11) on case histories will be included in the section of validation.

4.3 Determination of the Subsurface Settlement

In addition to the maximum ground surface settlement, subsurface settlements at different depths were collected from results of FEM analyses on artificial excavations. Both the shape and the magnitude of subsurface settlement troughs were rarely discussed before.

Amounts of the maximum subsurface settlements, S_m, at various depths were firstly investigated in the hypothetic cases. Ratios of the maximum subsurface settlement to the maximum ground surface settlement, S_m/δ_{vm}, are plotted against the normalized depth, D/H, in Fig. 12. Only data points from hypothetic cases with AR = 1.2 were plotted since data of different AR are almost coincide with each other. The ratios of S_m to δ_{vm} from results of FEM on the calibration case were also put in the figure. As observed in the figure, the S_m at depths between 0.1H to 0.4H is about 10% greater than the δ_{vm}. For conservative, ratio of S_m to δ_{vm} could be assumed to be 1.1 for depths

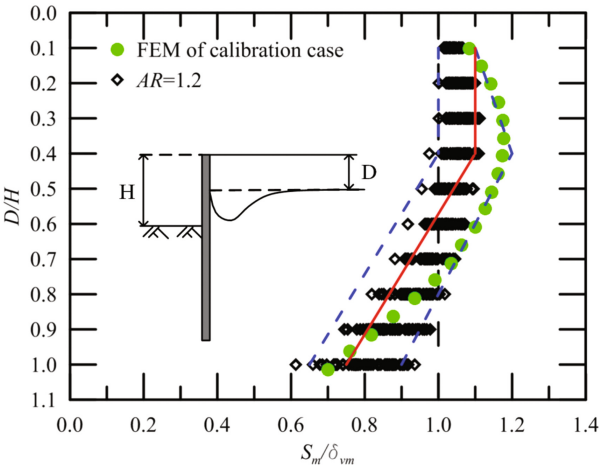

Fig. 12. Normalized subsurface settlement against normalized depth

above 0.4H. The ratio then reduced gradually to a final value of 0.75 at the depth of 1.0H. The upper/lower limits for the ratio of S_m to δ_{vm} were also plotted in the figure.

The profile of the subsurface settlement is as important as the determination of the maximum subsurface settlement. Hsieh and Ou (1998) proposed a concept of influence zones on the ground surface settlement due to excavation and a procedure for estimating the ground surface settlement profile. The profile is divided into two segments, i.e., the primary influence zone (*PIZ*) and secondary influence zone (*SIZ*), and could be determined once the δ_{vm} is known. The estimation of ground surface profile and determination of *PIZ* is modified by Ou and Hsieh (2011), which is based on the excavation depth (H), the excavation width (B), the depth of soft clay bottom (H_f), and the depth of the hard stratum (H_g). The proposed *PIZ* is shown in Fig. 13. The subsurface settlement profiles in selected representative hypothetic cases, which included various excavation depths, excavation widths, soil properties and structural stiffness, were plotted in Fig. 14. The subsurface settlement (S) at any distance behind the wall (d) is normalized by the maximum subsurface settlement (S_m) at the selected depth. For each of the selected hypothetic cases, the *PIZ* is calculated and used as a factor to normalize the distance (d). By observing the relationship between S/S_m and d/PIZ at any normalized depth (D/H), the ground settlement profiles are generally similar. The location of maximum settlements varied slightly from 1/3 to 1/4 of d/PIZ with the increase of depths; moreover, the settlement ratio (S/S_m) at position of $d = PIZ$ is reduced from 1/6 when D = 0 to 1/10 when D = 1.0H. However, in general, the settlement profile proposed by Ou and Hsieh (2011) still works quite well for those on the surface and subsurface. The reason could be that the PIZ is related to the strain induced by the excavation. For soils within the range of PIZ, both the subsurface settlement and the ground surface settlement were affected by the same mechanism.

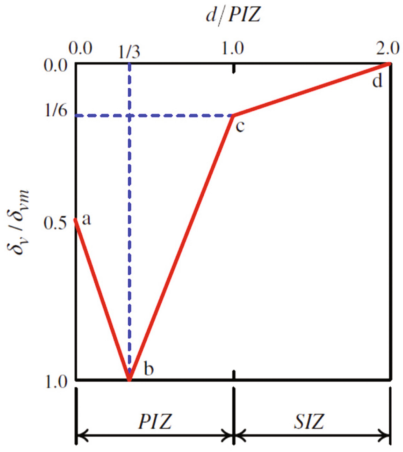

Fig. 13. Primary influence zone (reprint after Ou and Hsieh 2011)

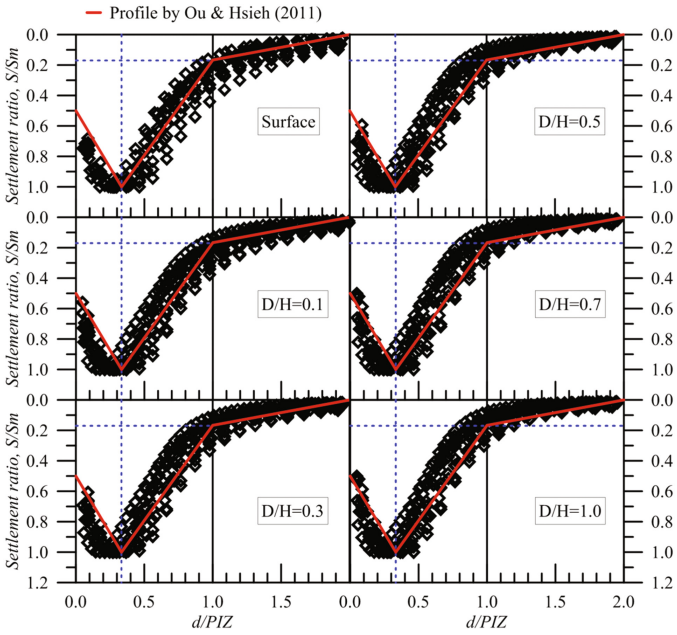

Fig. 14. Ground settlement profiles at different depths

Therefore, the subsurface settlement at any depth and distance behind the wall can be determined by applying Figs. 12, 13 and 14.

4.4 Summary of the Simplified Evaluation Method

The flowchart of the proposed simplified evaluation for ground movements is shown in Fig. 15 which included the following parts:

1. The simplified equation for determination of the maximum wall deflection based on parameters of H, B, s_u, S_w, S_a, and AR, i.e., Eqs. (4) and (5);
2. The simplified equation for determination of the maximum ground surface settlement based on parameters of H, B, s_u, S_w, S_a, and AR, i.e., Eqs. (9) and (10);
3. A quick assessment for the maximum wall deflection and the maximum ground surface settlement by Figs. 7 and 9
4. An additional evaluation equation for the maximum ground surface settlement based on the relationship between the maximum wall deflection and the maximum ground surface settlement, i.e., Eq. (11);
5. Simplified evaluation for the maximum value and profiles of the subsurface settlement, i.e., Figs. 12 and 14.

The simplified evaluation was obtained from multivariate regression analysis of numerical analyses on hypothetic excavations with: H = 10 to 30 m, B = 20 to 80 m, s_u/σ'_v = 0.28 to 0.34, S_w of diaphragm walls to sheet piles, S_a of steel struts and

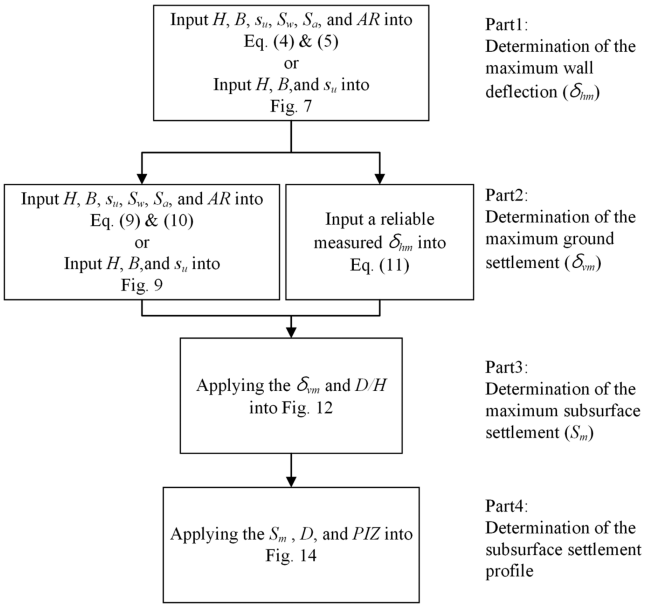

Fig. 15. Flowchart of the proposed simplified method

concrete floor slabs, and AR of isotropy and anisotropy. It should be noted the undrained shear strength used in the evaluations are that of axial compression under K_0-consolidation (CK_0U-AC). The average undrained shear strength used in isotropic analysis, similar to that obtained from the unconsolidated-undrained test (UU) or the FV test (field van shear), could be calculated by the following equation.

$$s_{u,avg} = \frac{s_{u,AC} + s_{u,AE}}{2} = \frac{s_{u,AC} + K_s s_{u,Ac}}{2} = \frac{(1 + K_s) s_{u,AC}}{2} \tag{12}$$

where $s_{u,iso}$ is the undrained strength in Mohr-Coulomb model; $s_{u,AC}$ is the undrained strength of axial compression; $s_{u,AE}$ is the undrained strength of axial extension; K_s is the anisotropic ratio of undrained strength.

Thus, the proposed simplified method should better be applied to the excavation which the dimension, soil properties, and stiffness of braces are in the above range.

5 Validation

Four case histories (Ou et al. 1998; Hsieh and Ou 2012) with detailed construction information were employed to validate the proposed simplified evaluation method. Table 3 lists the excavation geometry and subsoil properties used in the simplified evaluation. The anisotropic ratio of soil stiffness in case 1 was determined by test results (Teng et al. 2014), and ratios in other three cases were assumed to be equal to the average value of Taipei clay shown in Table 1. Intermediate stages in four cases

Table 3. Summary of excavation case histories

Case No.	B (m)	$\frac{s_u}{\sigma'_v}$	H_g (m)	Stage No.	H (m)	S_w	S_a (MN/m)	AR	α_g	observed δ_{hm} (mm)	observed δ_{vm} (mm)
1	38.2	0.33	46.0	4	11.8	638	2625	1.4	1.00	65	34
				5	15.2	732	2893	1.4	1.00	80	52
				6	17.3	1065	3054	1.4	1.00	99	68
				7	19.7	1313	2760	1.4	1.00	106	78
2	20.0	0.33	51.0	4	9.2	3065	3443	1.3	1.00	32	–
				5	11.7	3573	3017	1.3	1.00	41	–
				6	13.9	4495	2854	1.3	1.00	47	–
				7	16.2	4952	2745	1.3	1.00	55	–
3	62.4	0.34	32.0	3	12.4	179	2197	1.3	1.00	91	55
				4	15.4	285	2697	1.3	1.00	102	61
				5	16.9	562	2947	1.3	1.00	114	70
				6	20.0	598	3097	1.3	0.82	124	77
4	33.4	0.34	31.0	4	10.2	1239	1039	1.3	1.00	42	–
				5	13.2	1239	1307	1.3	1.00	49	–
				6	16.2	1255	1579	1.3	1.00	60	–
				7	18.5	1498	1761	1.3	0.89	63	43

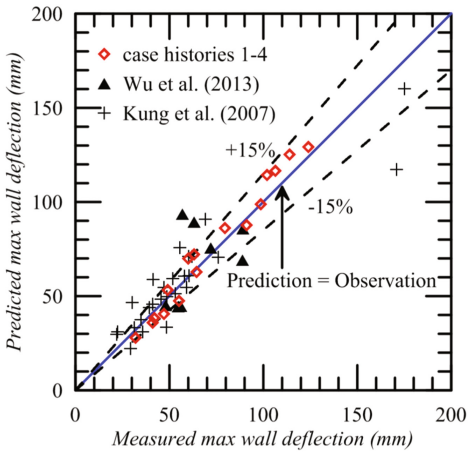

Fig. 16. Comparison between measured and calculated max wall deflections for case history 1–4

were treated as individual case histories, and the maximum wall deflection could be estimated by Eqs. (4) and (5). Further validations were made on additional 8 case histories (Wu et al. 2013) and 23 case histories (Kung et al. 2007).

Figure 16 shows the comparison of the maximum wall deflection between observations and predictions made by using Eq. (5). For δ_{hm} at intermediate stages and the

final stage predicted by Eq. (5) are generally close to the line of prediction = observation. This result shows that the Eq. (5) is applicable to predict δ_{vm} not only at the final stage but intermediate stages. The result proves that Eq. (5) can yield a satisfactory prediction on δ_{hm}, which generally located within a range of $\pm 15\%$ of observed δ_{hm}.

In addition to the validation of prediction on δ_{hm}, the observed maximum ground surface settlements in case 1, 3 and 4 as listed in Table 3, and those in additional four case histories collected by Kung et al. (2007) were used for the validation of predicting the δ_{vm}. There are three evaluation methods presented hereinbefore, i.e., by Eqs. (10) and (11). Equation (10) was employed in calculating the maximum ground surface settlement at all stages. Equation (11) calculated the δ_{vm} based on the observed δ_{hm}/H. The comparison between observed and calculated δ_{hm} by three different methods are shown in Fig. 17. The performance of Eq. (10) is better than that of Eq. (11), since more factors such as excavation geometry and subsoil properties were considered in Eq. (10). However, the prediction results of Eqs. (10) and (11) are generally rational

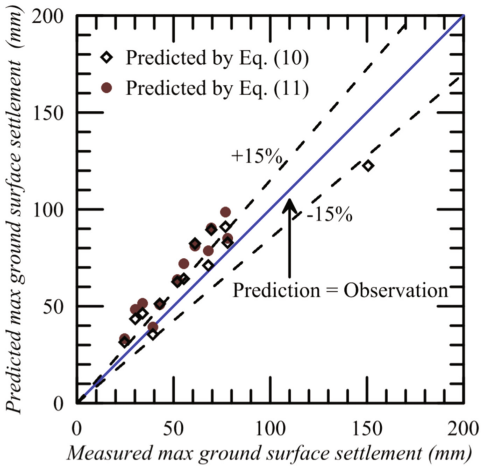

Fig. 17. Comparison between measured and calculated max ground surface settlement

Table 4. Estimated maximum subsurface settlement for case history 1

D (m)	*D/H*	S_m/δ_{vm}	δ_{vm} (mm)	S_m (mm)	*d/PIZ*		
8.0	0.41	1.10	78	85.8	0.05	0.20	0.41
12.0	0.61	1.00	78	78.0			
16.5	0.84	0.85	78	66.3			
20.0	1.02	0.75	78	58.5			

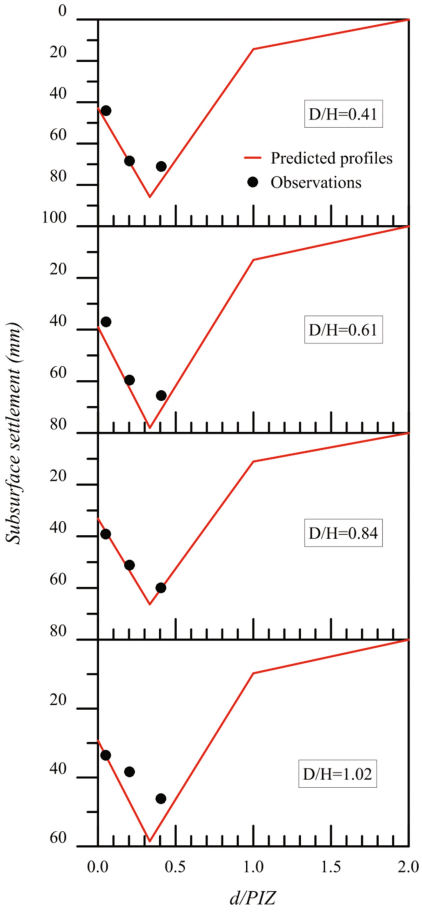

Fig. 18. Prediction for subsurface settlements in case history 1

and close to the range of 0.85 to 1.15 times observed value. The proposed evaluation methods for the maximum ground surface settlement are satisfactory with the above validation.

Validations of quick evaluation method for the maximum wall deflection and the maximum ground surface settlement are shown in Figs. 7 and 9. For the quick assessment of the maximum wall deflection, case histories with B = 20–80 m were employed. Although the prediction is not as accurate as that by Eq. (5), the results in Fig. 7 still demonstrate a satisfactory quick assessment prior to detail simulations on FEM. For the quick evaluation of the maximum ground surface settlement, five case histories with different undrained strength and excavation width are applied. The prediction results are generally sufficient for the initial assessment in the field when the engineer has limited information.

The prediction for subsurface settlement was validated through the case history 1 where the subsurface settlements were measured. The subsurface settlement was

monitored by extensometers, placed at 2 m, 8 m, and 16 m behind the wall, at depths of 8 m, 12 m, 17.5 m, and 20 m. The primary influence zone (*PIZ*) for case history 1 was calculated to be 39.4 m (Ou and Hsieh 2011). To estimate the subsurface settlement, the magnitude of the maximum subsurface settlements should be determined firstly by applying the *D/H* into Fig. 12. The estimated maximum subsurface settlements at different depths are listed in Table 4. Once the S_m is determined, the subsurface settlement profile can be plotted. The comparison of subsurface settlement between field observations and prediction profiles is shown in Fig. 18. The predicted settlement profiles matched the observations quite well at all depths and positions. It demonstrates the accuracy of the proposed evaluation method for determining the subsurface settlement.

6 Conclusion

35 case histories were employed to validate the prediction of maximum wall deflection. Of these case histories, four are well-documented case histories with detail construction information at all stages. The simplified equation for evaluating the maximum ground surface settlement was validated through seven case histories. The computed maximum wall deflections and maximum ground surface settlements were generally in good agreement with the field observations. The proposed simplified evaluation provided a quick and reliable assessment of ground movements induced by excavation. In addition, a quick evaluation method for both wall deflections and ground surface settlements based on soil strength and excavation geometry were proposed and validated. It provides an initial assessment for engineers in the field with limited information.

The evaluation for damage potential of buildings adjacent to a braced excavation should base on the subsurface settlement profile. An evaluation method for the subsurface settlement, including the magnitude and shape, was suggested herein. The maximum subsurface settlement at a depth less than 0.4H was possibly greater than the ground surface settlement for 10% to 20%. The maximum subsurface settlement at depth deeper than 0.4H decreased gradually to an average value of $0.75S_m$ at the depth of 1.0H. For the shape of the subsurface settlement, the location of maximum settlements varied slightly from 1/3 to 1/4 of *d/PIZ* with the increase of depths, and the settlement ratio (S/S_m) at position of $d = PIZ$ is reduced from 1/6 to 1/10 at depth of 1.0H. However, the subsurface settlement profiles are generally similar to that on the ground surface. The settlement profile proposed by Ou and Hsieh (2012) is thus suggested. A case history that monitored the subsurface settlements at various depths and distances was employed to validate the proposed method. The result shows a good agreement between predictions and observations which implied the subsurface settlement could be well predicted by the proposed evaluation method.

References

Atkinson, J.H., Sallfors, G.: Experimental determination of soil properties. In: Proceedings of 10th ECSMFE, Florence, vol. 3, pp. 915–956 (1991)

Benz, T.: Small-strain stiffness of soils and its numerical consequences. Ph.D. dissertation, University Stuttgart, Germany (2007)

Bowles, J.E.: Foundation Analysis and Design, 4th edn. McGraw-Hill, New York (1986)

Burland, J.B.: Ninth Laurits Bjerrum Memorial Lecture. 'Small is beautiful'. The stiffness of soils at small strains. Can. Geotech. J. **26**(4), 499–516 (1989)

Cho, W., Finno, R.J.: Stress-strain responses of block samples of compressible chicago glacial clays. J. Geotech. Geoenviron. Eng. **136**(1), 178–188 (2010)

Clough, G.W., O'Rourke, T.D.: Construction-induced movements of in-situ walls. In: Proceedings, Design and Performance of Earth Retaining Structure, ASCE Special Conference, Ithaca, New York, pp. 439–470 (1990)

Duncan, J.M., Chang, C.Y.: Nonlinear analysis of stress and strain in soils. J. Soil Mech. Found. Div. ASCE **96**(5), 637–659 (1970)

Hashash, Y.M.A., Whittle, A.J.: Ground movement prediction for deep excavations in soft clay. J. Geotechn. Geoenviron. Eng. **122**(6), 474–486 (1996)

Hashash, Y.M.A., Whittle, A.J.: Mechanisms of load transfer and arching for braced excavations in clay. J. Geotech. Geoenviron. Eng. **128**(3), 187–197 (2002)

Hsieh, P.G., Ou, C.Y.: Shape of ground surface settlement profiles caused by excavation. Can. Geotech. J. **35**(6), 1004–1017 (1998)

Hsieh, P.G.: Prediction of maximum ground movements induced by deep excavation in clay. J. Chin. Inst. Civil Hydraul. Eng. **13**(3), 489–498 (2001). (in Chinese)

Hsieh, P.G., Ou, C.Y.: Analysis of nonlinear stress and strain in clay under the undrained condition. J. Mech. **27**(2), 201–213 (2011)

Hsieh, P.G., Ou, C.Y.: Analysis of deep excavations in clay under the undrained condition with small strain characteristics. J. Chin. Inst. Eng. **35**(5), 601–616 (2012)

Jardine, R.J., Potts, D.M., Fourie, A.B., Burland, J.B.: Studies of the influence of non-linear characteristics in soil-structure interaction. Geotechnique **36**(3), 377–396 (1986)

Kung, T.C., Juang, C.H., Hsiao, C.L., Hashash, Y.M.A.: Simplified model for wall deflection and ground surface settlement caused by braced excavation in clays. J. Geotech. Geoenviron. Eng. **133**(6), 731–747 (2007)

Lee, K.M., Rowe, R.K.: Deformations caused by surface loading and tunneling: the role of elastic anisotropy. Geotechnique **39**(1), 125–140 (1989)

Mana, A.I., Clough, G.W.: Prediction of movements for braced cuts in clay. J. Geotech. Eng. ASCE **107**(6), 759–777 (1981)

Mesri, G., Huvaj, N.: Shear strength mobilized in undrained failure of soft clay and silt deposits. ASCE Geotechnical Special Publication 173, Geo-Denver (2007)

Ng, C.W.W., Leung, E.H.Y., Lau, C.K.: Inherent anisotropic stiffness of weathered geomaterial and its influence on ground deformations around deep excavations. Can. Geotech. J. **41**(1), 12–24 (2004)

Ou, C.Y., Heish, P.G., Chiou, D.C.: Characteristics of ground surface settlement during excavation. Can. Geotech. J. **30**(5), 758–767 (1993)

Ou, C.Y., Hsieh, P.G.: A simplified method for predicting ground settlement profiles induced by excavation in soft clay. Comput. Geotech. **38**(8), 987–997 (2011)

Peck, R.B.: Deep excavation and tunneling in soft ground. In: Proceedings of the 7th International Conference on Soil Mechanics and Foundation Engineering, State-of-the-art volume, Mexico City, pp. 225–290 (1969)

Simpson, B., Ng, C.W.W.: Anisotropic analysis of settlement trough due to tunnelling in an overconsolidated clay. In: Proceedings of the 10th Asian Regional Conference on Soil Mechanics and Foundation Engineering, vol. 2, pp. 166–167. International Academic Publisher, Beijing (1995)

Teng, F.C., Ou, C.Y., Hsieh, P.G.: Measurements and numerical simulations of the inherent stiffness anisotropy in soft Taipei clay. J. Geotech. Geoenviron. Eng. **140**(1), 237–250 (2014)

Whittle, A.J., Kavvadas, M.J.: Formulation of the MIT-E3 constitutive model for overconsolidated clays. J. Geotech. Eng. ASCE **120**(1), 173–198 (1994)

Whittle, A.J., Degroot, D.J., Ladd, C.C., Seah, T.H.: Model prediction of anisotropic behavior of Boston blue clay. J. Geotech. Eng. ASCE **120**(1), 199–224 (1994)

Wong, K.S., Broms, B.B.: Lateral wall deflections of braced excavations in clay. J. Geotech. Eng. ASCE **115**(6), 853–870 (1989)

Wu, S.H., Ching, J., Ou, C.Y.: Predicting wall displacements for excavations with cross walls in soft clay. J. Geotech. Geoenviron. Eng. **139**(6), 914–927 (2013)